Supporting Information

Towards zero bias photoelectrochemical water splitting: onset potential improvement of Mg:GaN-modified Ta_3N_5 photoanode

Ela Nurlaela,[a] Yutaka Sasaki,[a] Mamiko Nakabayashi,[b] Naoya Shibata,[b] Taro Yamada,[a] and Kazunari Domen*[a]

Abstract: Tantalum nitride (Ta_3N_5) based photoanodes were overlaid with magnesium-doped gallium nitride (Mg:GaN) thin films by plasma-enhanced chemical vapor deposition (PCVD) technique, and subjected to photoelectrochemical activity tests, aiming for a negative shift of onset potential for O_2 evolution. A remarkable negative shift of the onset potential was observed after annealing Mg:GaN in N_2 gas, reaching 0 V vs RHE, despite a lower photocurrent than that on bare Ta_3N_5. Mg:GaN annealed in NH_3 exhibited an improvement of the photocurrent. A detailed study of the photoelectrochemical performance for various samples and a thorough characterization have revealed the effects of N_2/NH_3 post annealing over Mg activation/Ta_3N_5 damage recovery, controlling the onset potential shift and the current density improvement. N_2 post annealing shifted the onset potential to 0 V vs RHE but decreased the current density. On the other hand, NH_3 post annealing slightly shifted the onset potential and increased the current density largely. Albeit the current density loss, this onset potential shift unlocks the prospect of unassisted photoelectrochemical water splitting on Ta_3N_5.

[a] Dr. E. Nurlaela, Y. Sasaki, Dr. T. Yamada, Prof. K. Domen
School of Engineering, the University of Tokyo , 7-3-1 Hongo, Bunkyo-ku, Tokyo 113-8656 (Japan)

Japan Technological Research Association of Artificial Photosynthetic Chemical Process, 2-11-9 Iwamotocho, Chiyoda-ku, Tokyo 101-0032 (Japan)
E-mail: domen@chemsys.t.u-tokyo.ac.jp

[b] M. Nakabayashi, Prof. N. Shibata
Institute of Engineering Innovation, The University of Tokyo,2-11-16 Yayoi, Bunkyo-ku, Tokyo 113-8656 (Japan)

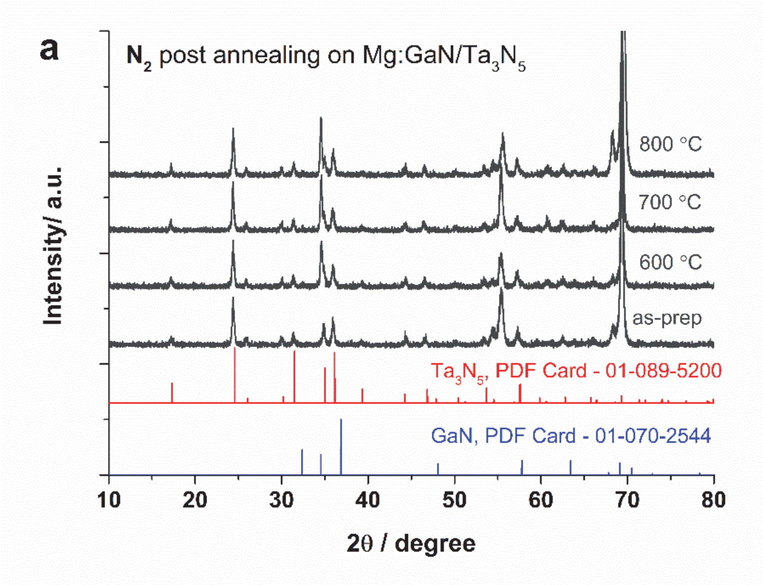

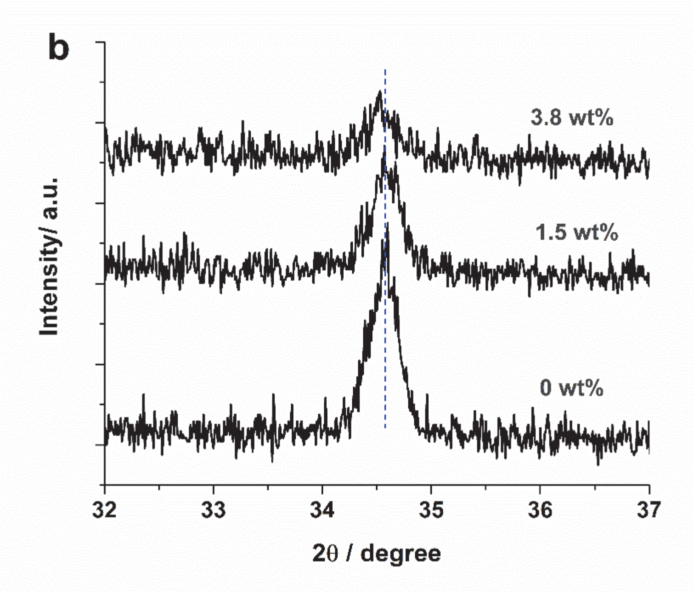

Figure S1. XRD patterns of a) Mg:GaN/Ta_3N_5 with different Mg:GaN thickness, b) Mg:GaN/Pyrex glass with different Mg concentration.

Table S1. EDS elemental analysis of Mg:GaN/Ta_3N_5 sample before and after post annealing in N_2 or NH_3.

Elements	Concentration, wt%		
	As-prepared	N_2-post annealed	NH_3-post annealed
Mg	2.2	2.0	0.7
Ga	76.2	76.6	70.4
N	14.5	14.9	12.9
O	3.9	3.2	1.5
Ta	3.2	3.5	14.5
Total	100.0	100.0	100.0

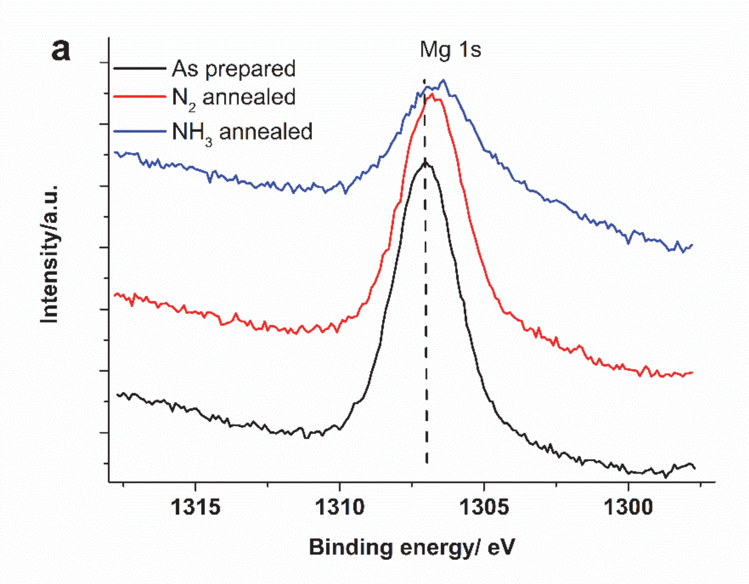

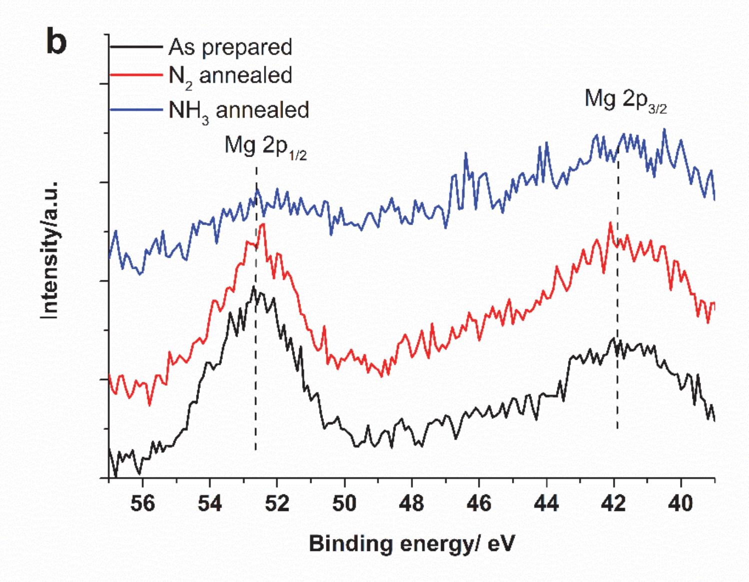
b
As prepared
N2 annealed
NH3 annealed
Mg 2p1/2
Mg 2p3/2
Intensity/a.u.
56 54 52 50 48 46 44 42 40
Binding energy/ eV

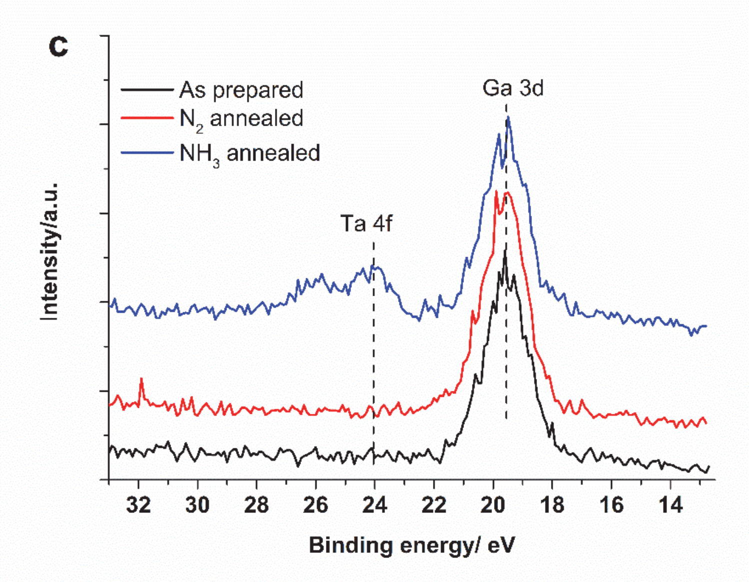
c
As prepared
N2 annealed
NH3 annealed
Ga 3d
Ta 4f
Intensity/a.u.
32 30 28 26 24 22 20 18 16 14
Binding energy/ eV

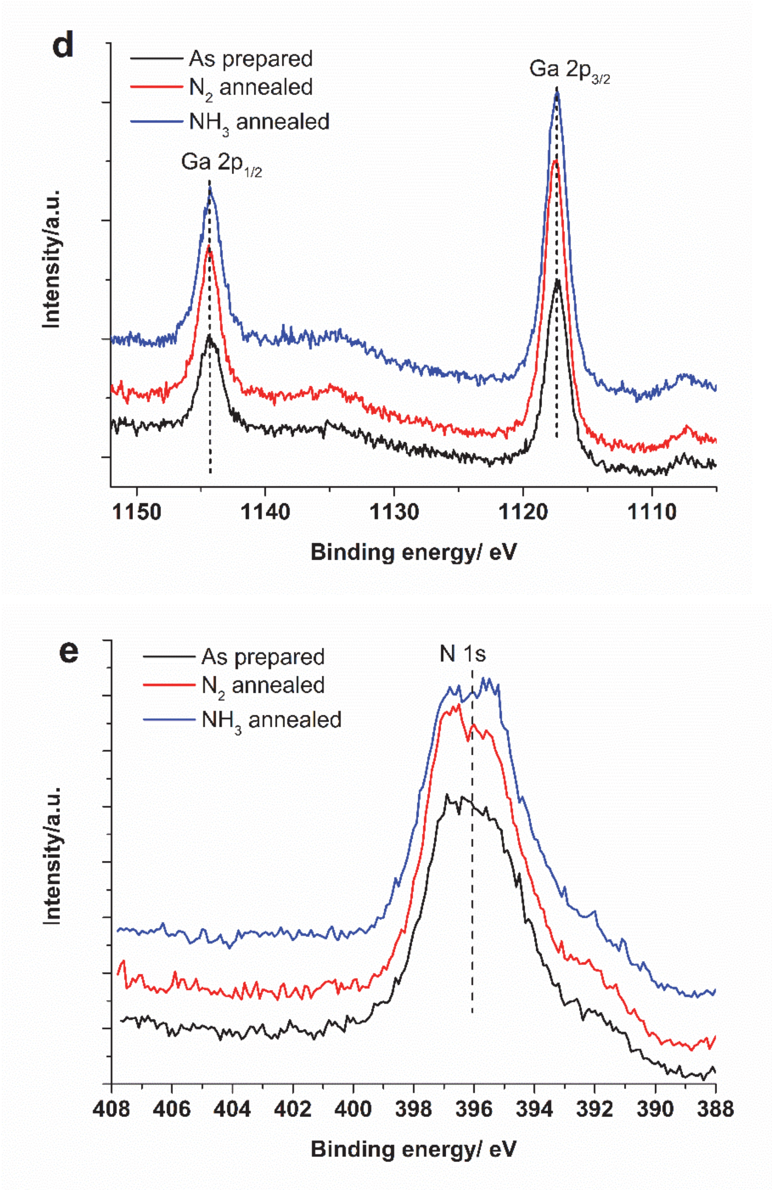

d
As prepared
N2 annealed
NH3 annealed
Ga 2p1/2
Ga 2p3/2
Intensity/a.u.
1150
1140
1130
1120
1110
Binding energy/ eV
e
As prepared
N2 annealed
NH3 annealed
N 1s
Intensity/a.u.
408
406
404
402
400
398
396
394
392
390
388
Binding energy/ eV

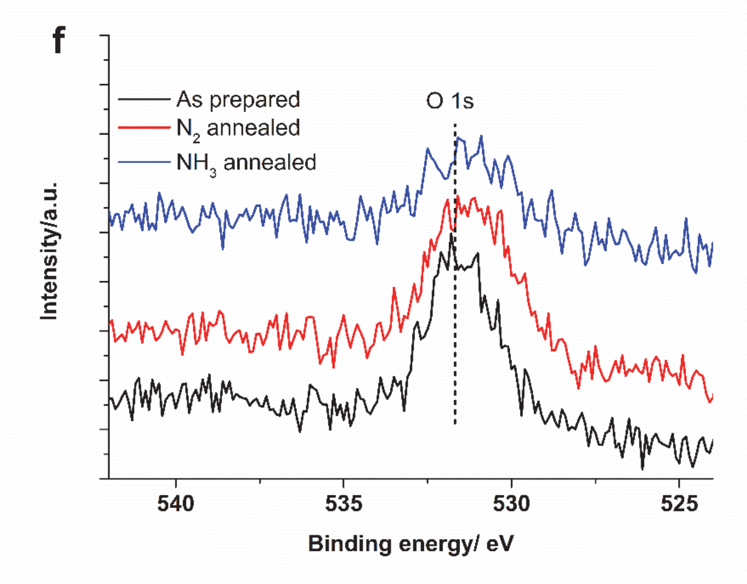

f
As prepared
N_2 annealed
NH_3 annealed
O 1s
Intensity/a.u.
540
535
530
525
Binding energy/ eV

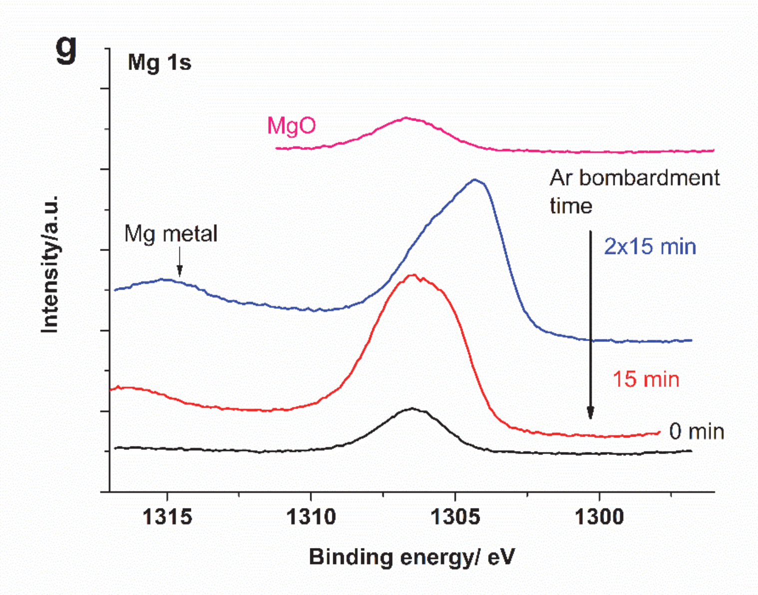

g
Mg 1s
MgO
Ar bombardment time
Mg metal
2x15 min
15 min
0 min
Intensity/a.u.
1315
1310
1305
1300
Binding energy/ eV

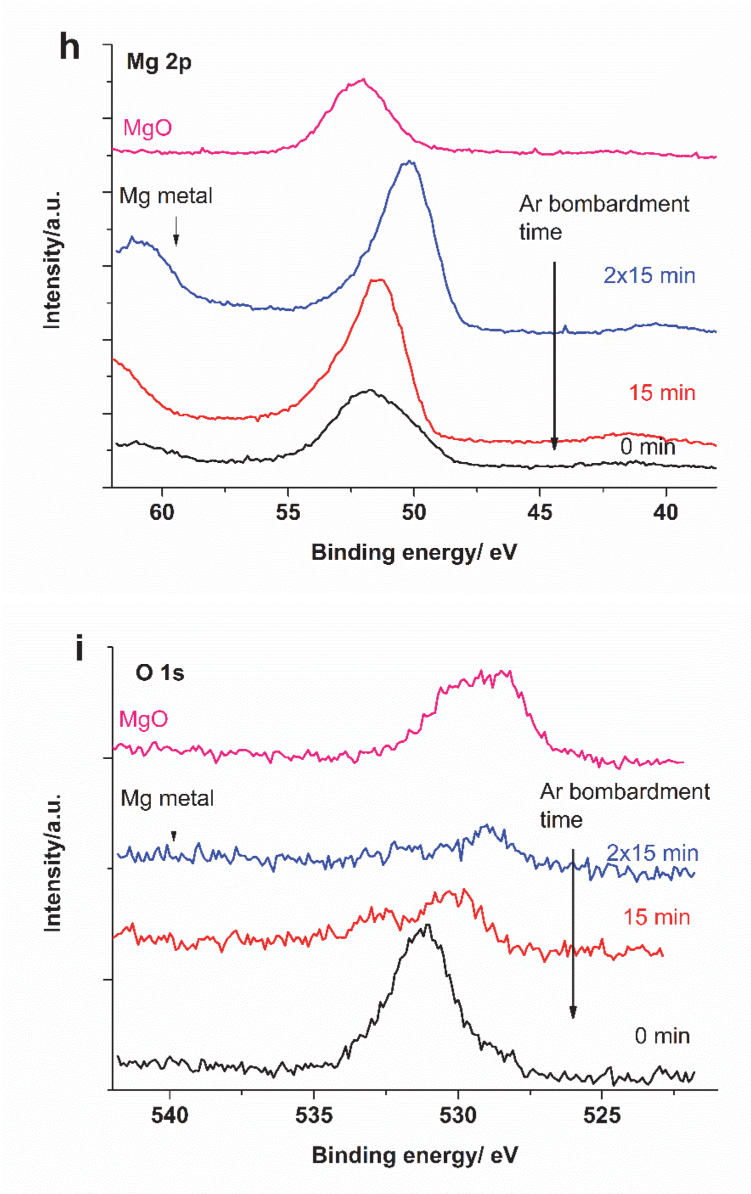

Figure S2.

a – f : XPS elemental peaks of Mg:GaN/Ta_3N_5 sample surfaces as prepared, post-annealed in N_2, and post-annealed in NH_3.

g – i : XPS elemental peaks for standard Mg materials. Mg 1s, Mg 2p and O 1s signals on MgO and Mg metal (Ar-bombarded for 15 min and 30 min for cleaning).

The Ga 2p3/2 peaks in d are positioned at 1117.5 eV of the binding energy, closely to that of typical GaN films grown by thermal CVD.[23]

Mg 1s peaks in a and b are positioned at that of oxidized Mg^{2+} (compared to g and h).

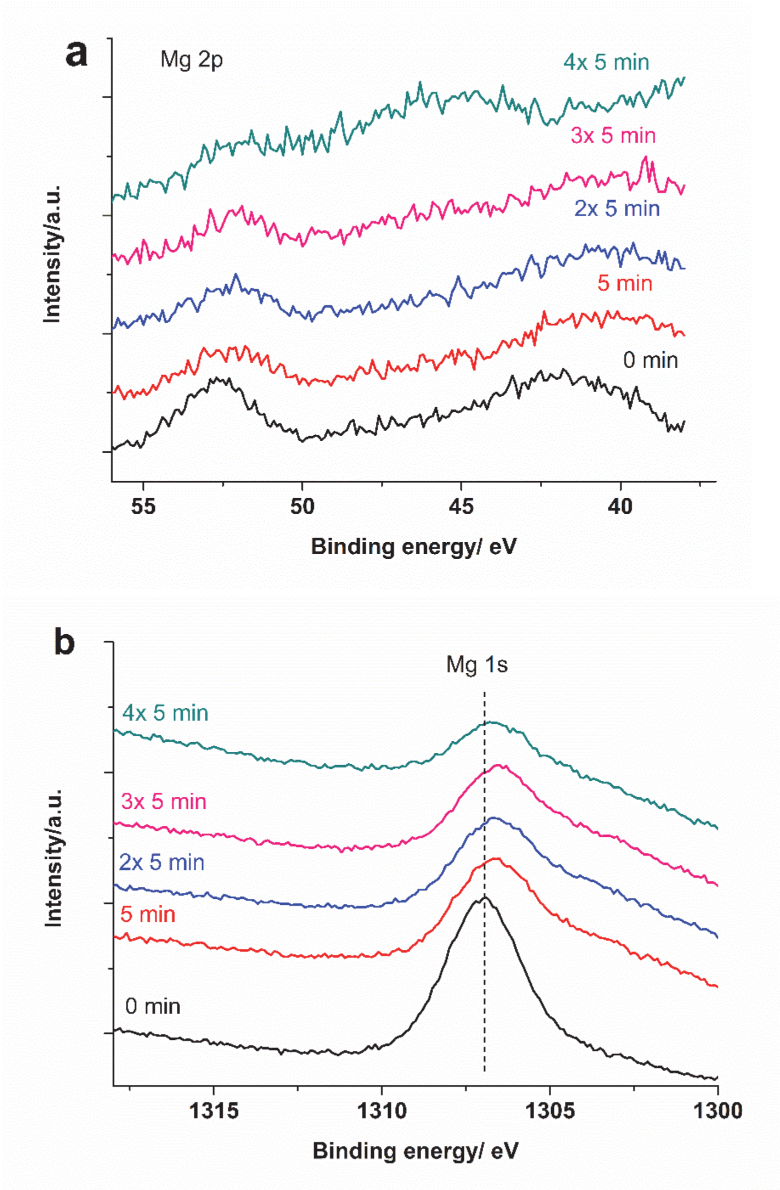
a
Mg 2p
4x 5 min
3x 5 min
2x 5 min
5 min
0 min
Intensity/a.u.
55
50
45
40
Binding energy/ eV
b
Mg 1s
4x 5 min
3x 5 min
2x 5 min
5 min
0 min
Intensity/a.u.
1315
1310
1305
1300
Binding energy/ eV

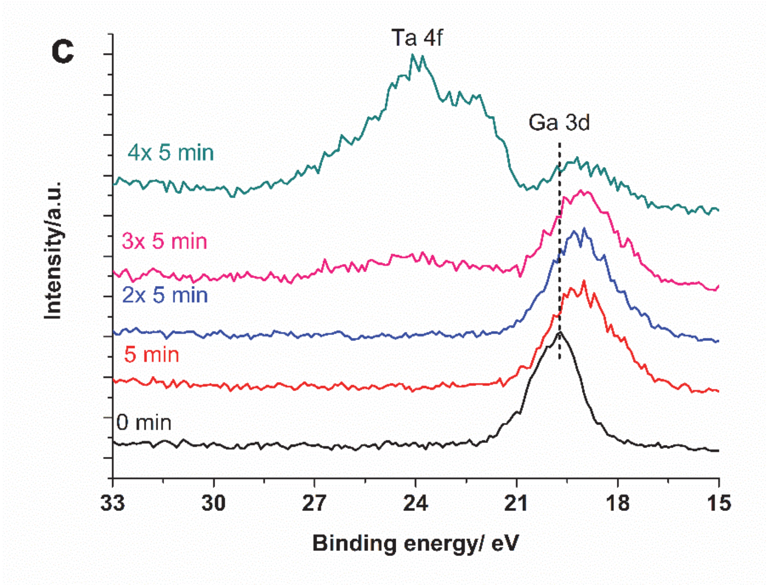
c
Ta 4f
Ga 3d
4x 5 min
3x 5 min
2x 5 min
5 min
0 min
Intensity/a.u.
33
30
27
24
21
18
15
Binding energy/ eV

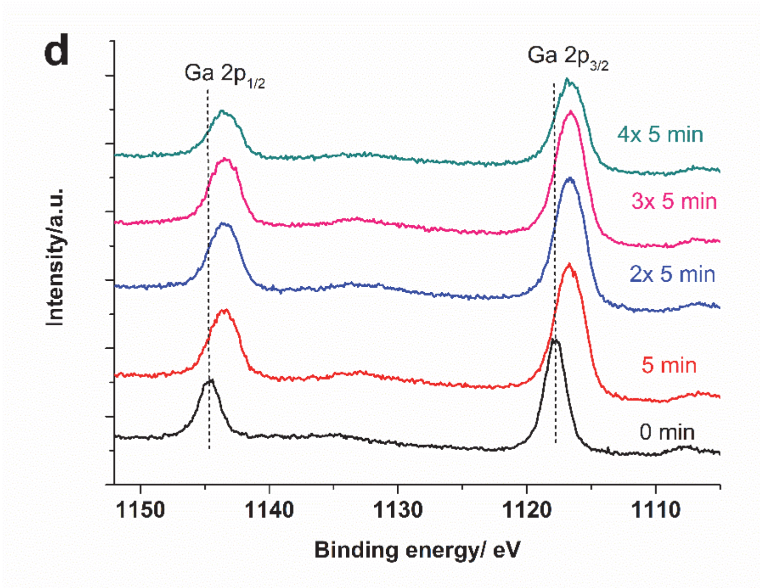
d
Ga $2p_{1/2}$
Ga $2p_{3/2}$
4x 5 min
3x 5 min
2x 5 min
5 min
0 min
Intensity/a.u.
1150
1140
1130
1120
1110
Binding energy/ eV

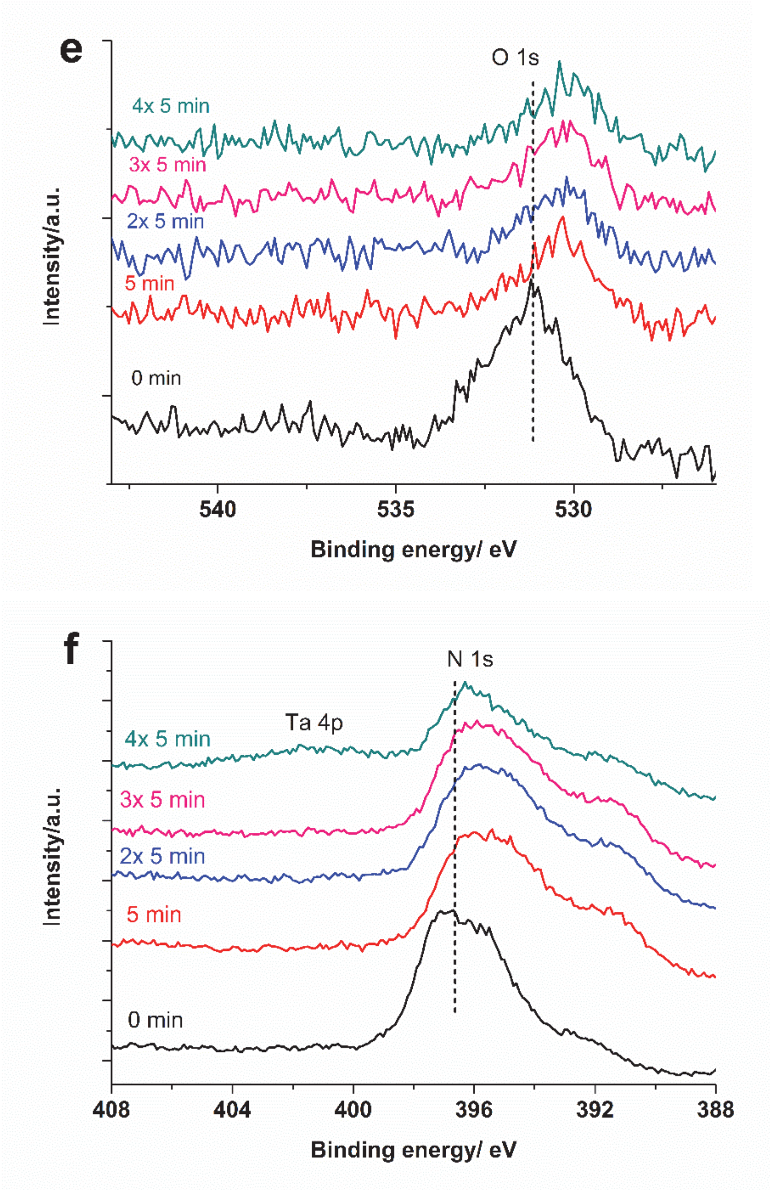

Figure S3. XPS of a) Mg 2p, b) Mg 1s, c) Ga 3d, d) Ga 2p, e) O 1s, f) N 1s on depth profiling of N_2 post annealed-Mg:GaN/Ta_3N_5.

Table S2. EDS elemental analysis of Mg:GaN area in Mg:GaN/Ta_3N_5 sample after N_2 post annealing.

Elements	Concentration, wt%
Mg	1.3
Ga	71.6
N	0.2
O	18.2
Ta	8.7
Total	100.0

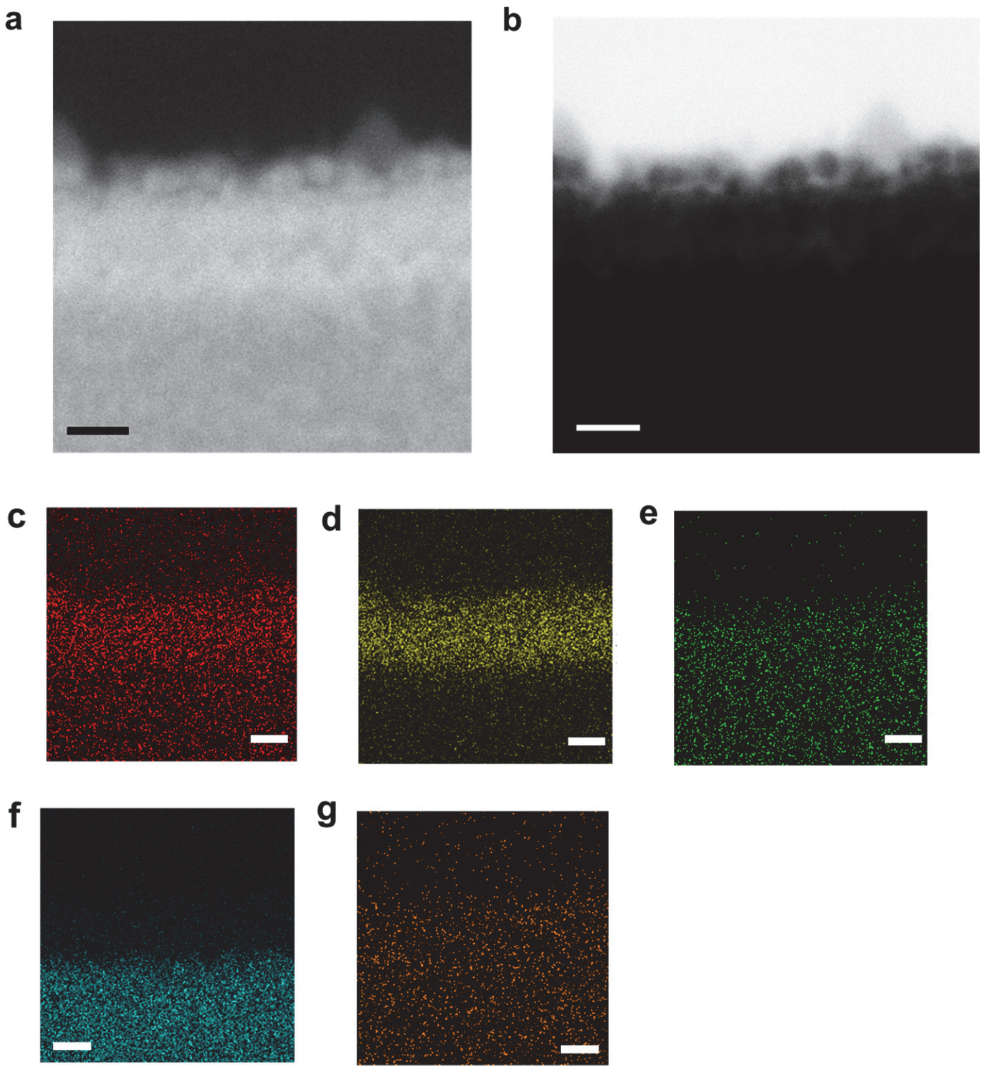

Figure S4. a) Dark- and b) bright-field cross-sectional STEM images of as-prepared Mg:GaN/Ta_3N_5 and STEM-EDS mapping of c) Mg, d) Ga, e) N, f) Ta, and g) O for the same observing area. Scale bar = 50 nm.

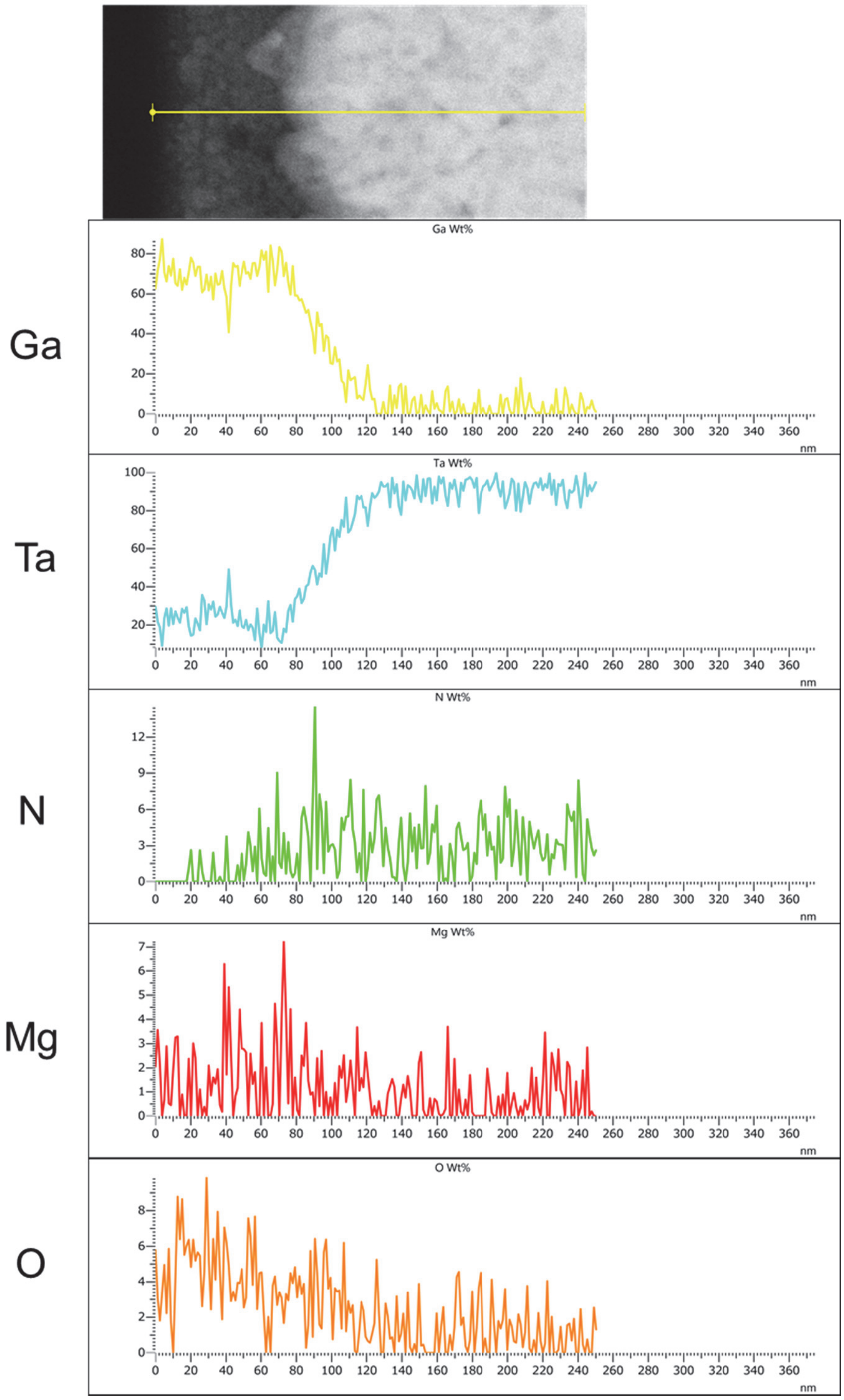

Figure S5. EDS line scan of the Mg:GaN/Ta_3N_5 after N_2 post annealing. The abscissa of each viewgraph corresponds to the position on the yellow line in the SEM image. The coordinate of each viewgraph indicates EDS counts (in an arbitrary unit).

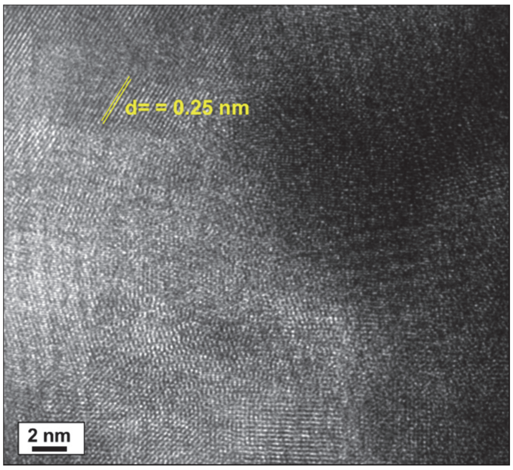

Figure S6. HRTEM image at interface of Ta_3N_5 (dark, right side) and Mg:GaN (bright, left side) after N_2 post annealing. The spacing of 0.25 nm in the striped pattern in the GaN side matches the (002) plane spacing of wurtzite GaN. This part of GaN agrees with the XRD pattern (Fig. 2) involving the intense peak at 2θ = 34.5°.

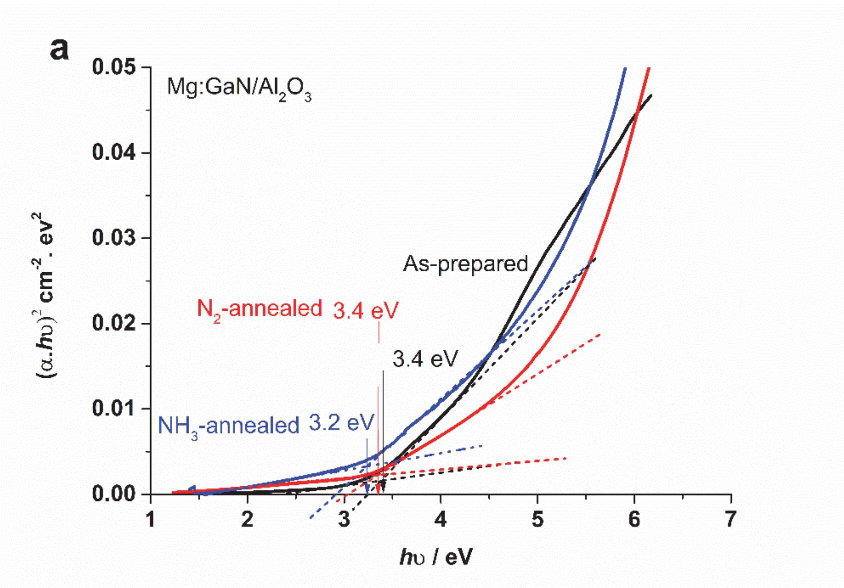

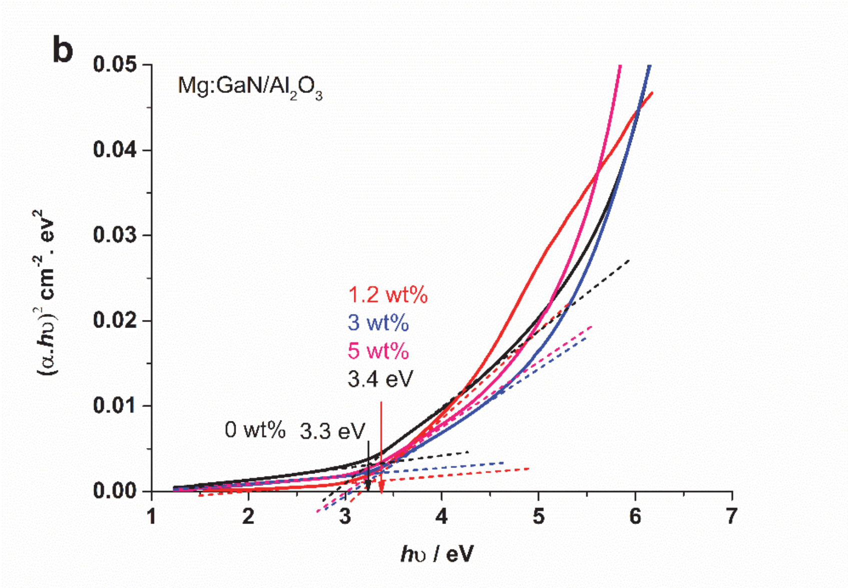

Figure S7. Tauc's plot of Mg:GaN/Al_2O_3 a) before and after post annealing, and b) with different Mg concentration. The Tauc's plot are used to determine the bandgap energy of the corresponding samples.

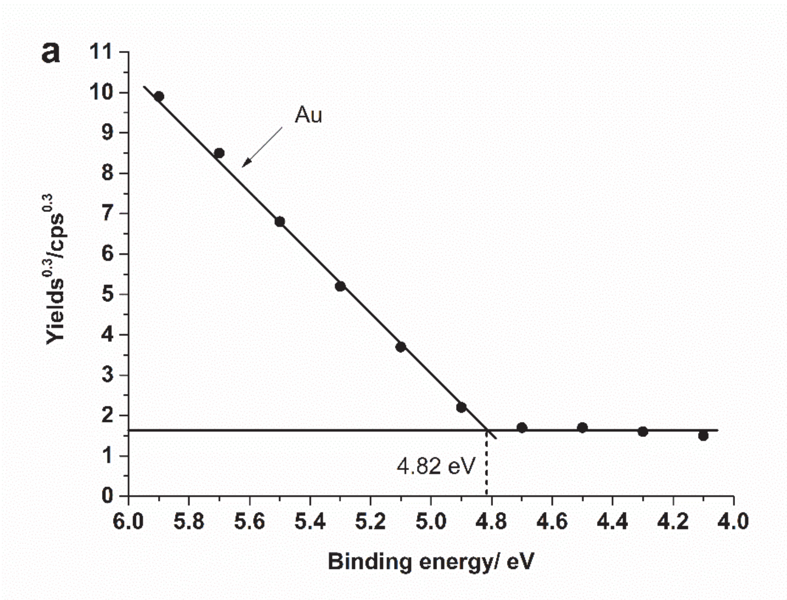

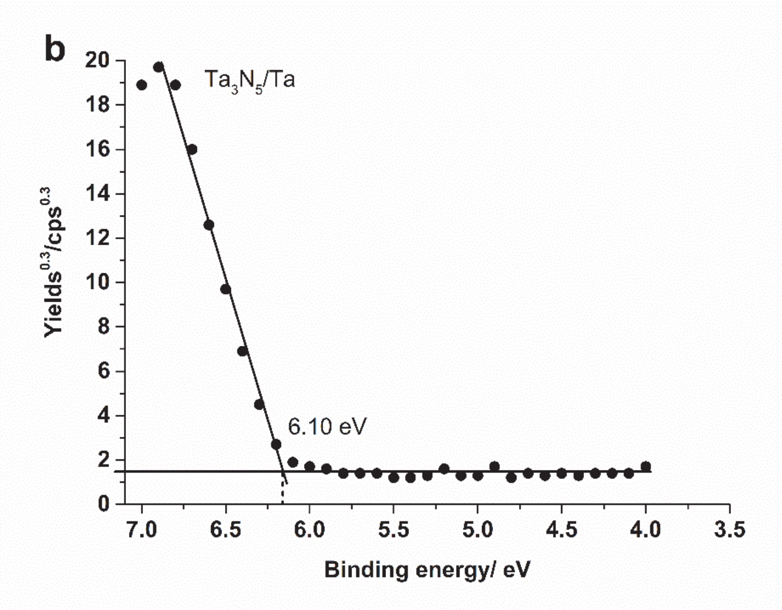
b
Ta3N5/Ta
6.10 eV
Yields0.3/cps0.3
Binding energy/ eV

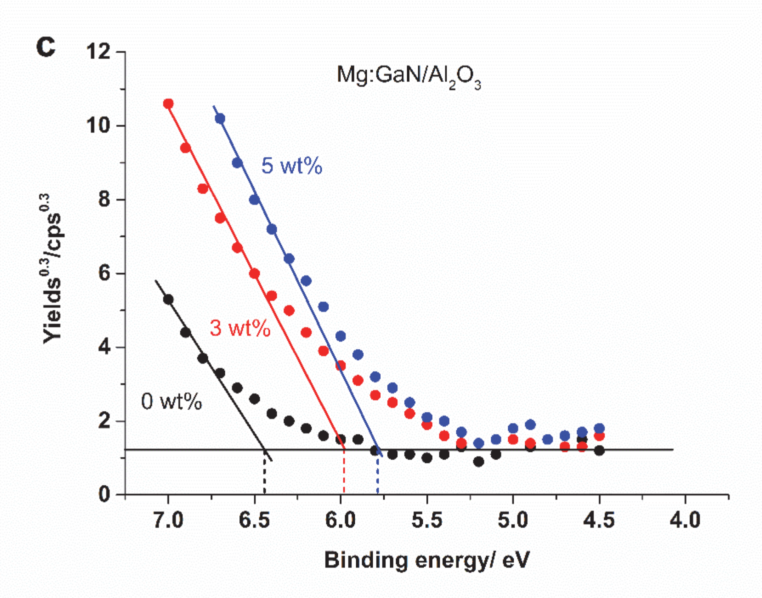
c
Mg:GaN/Al2O3
5 wt%
3 wt%
0 wt%
Yields0.3/cps0.3
Binding energy/ eV

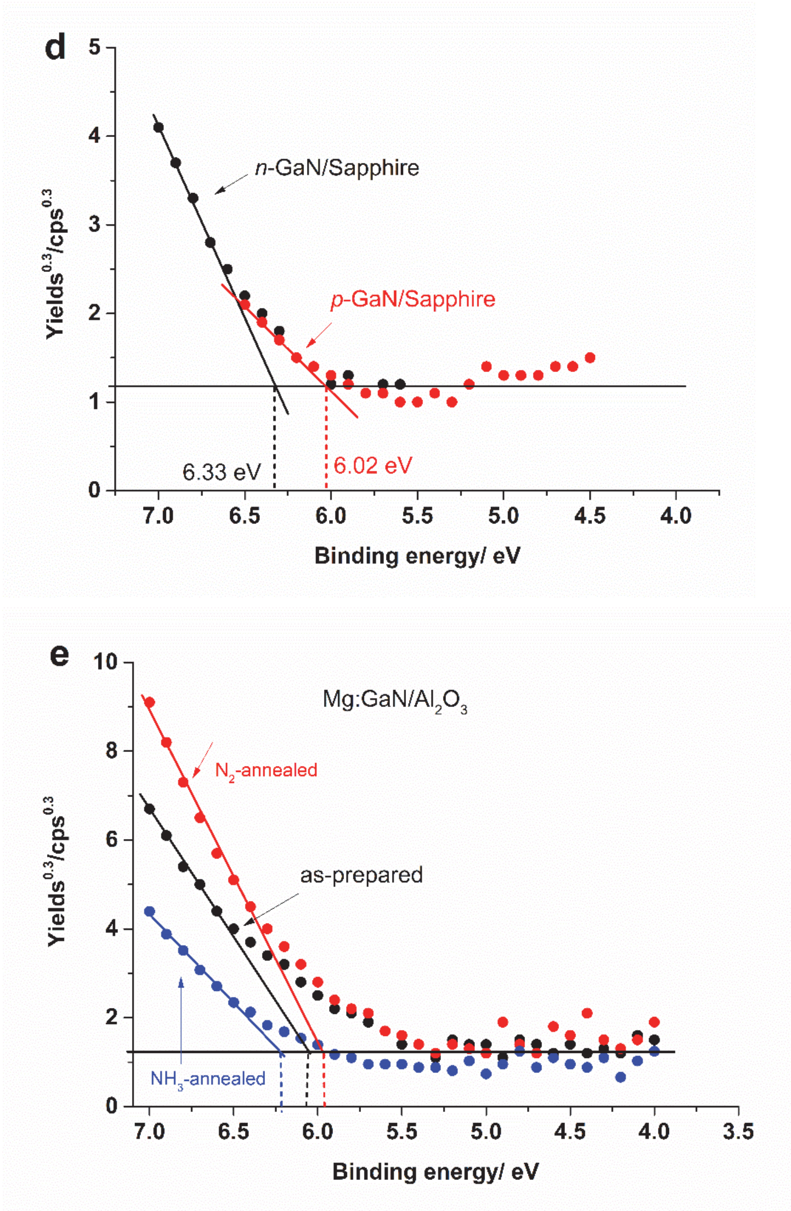

Figure S8. PESA spectra of a) Au, b) Ta_3N_5, c) Mg:GaN/Al_2O_3 with different Mg concentration, d) commercial *n*-GaN/sapphire and *p*-GaN/sapphire, and e) Mg:GaN/Al_2O_3 before and after post annealing.

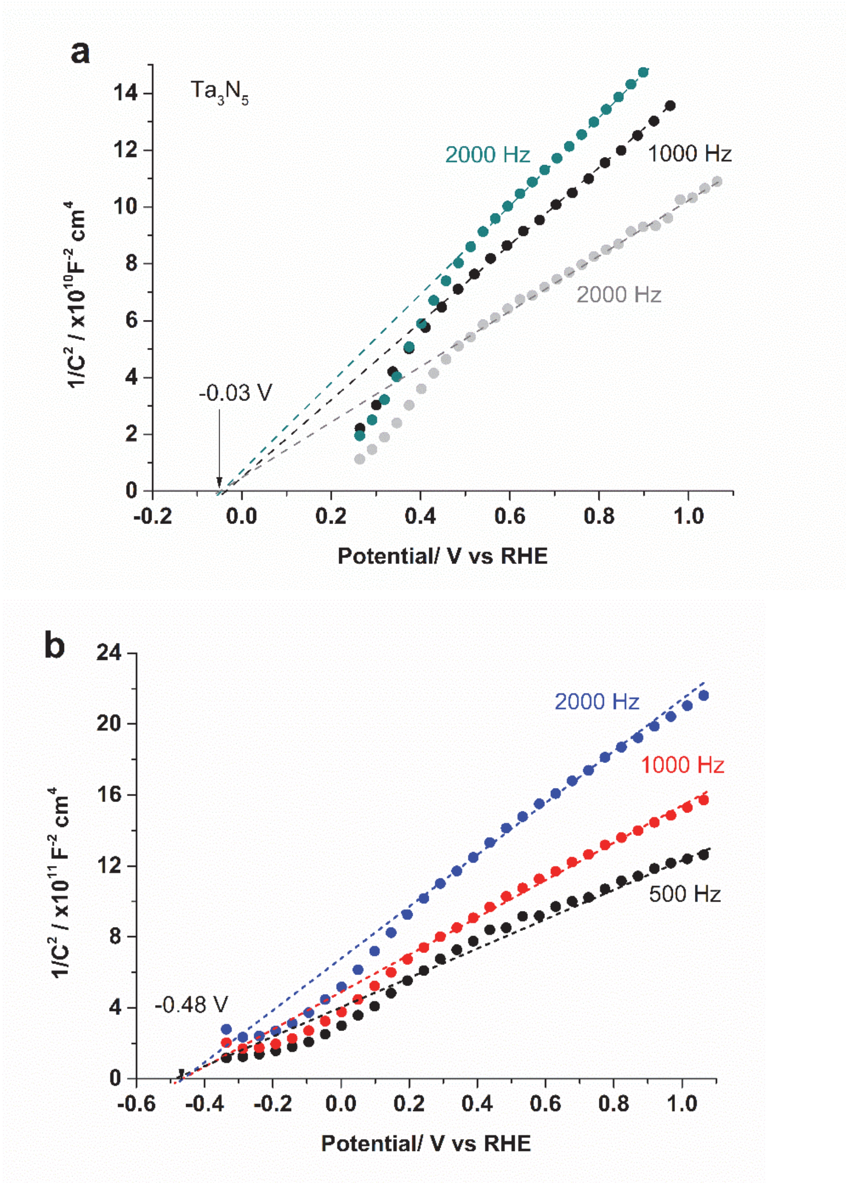
a
Ta_3N_5
2000 Hz
1000 Hz
2000 Hz
-0.03 V
$1/C^2$ / $x10^{10}F^{-2}$ cm^4
Potential/ V vs RHE
b
2000 Hz
1000 Hz
500 Hz
-0.48 V
$1/C^2$ / $x10^{11}$ F^{-2} cm^4
Potential/ V vs RHE

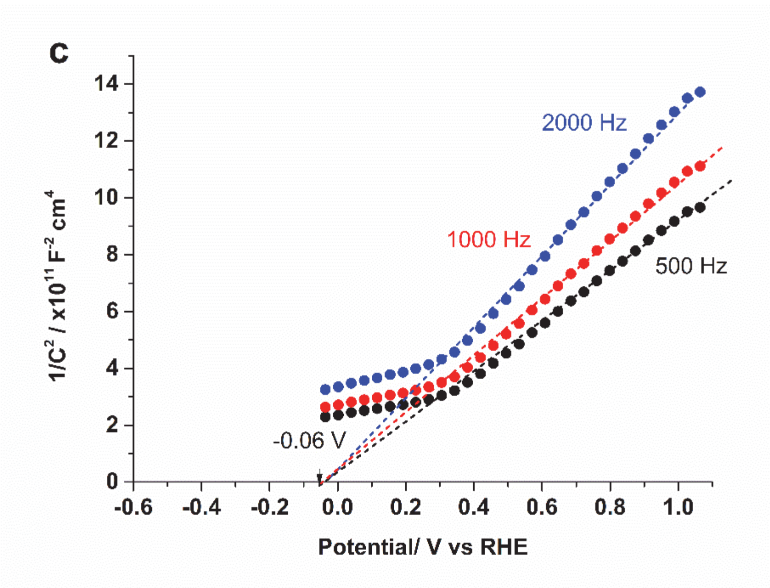
c
14
12
10
8
6
4
2
0
1/C² / x10¹¹ F⁻² cm⁴
2000 Hz
1000 Hz
500 Hz
-0.06 V
-0.6
-0.4
-0.2
0.0
0.2
0.4
0.6
0.8
1.0
Potential/ V vs RHE

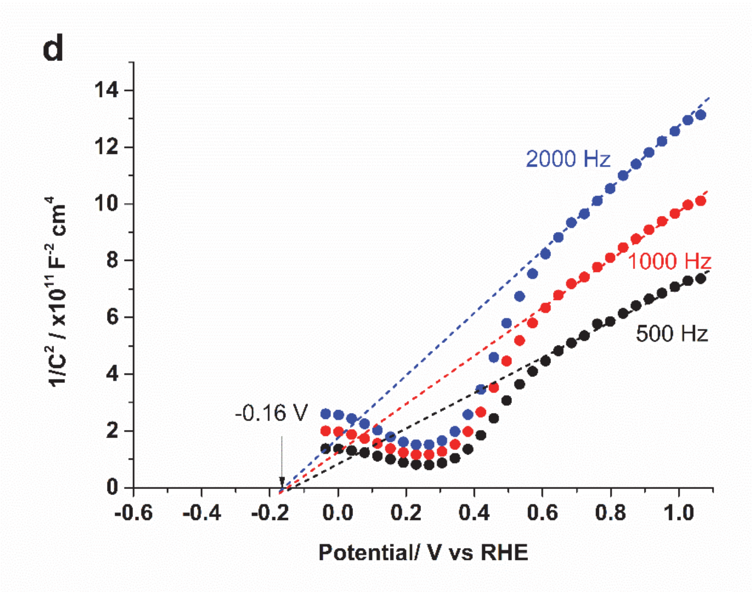
d
14
12
10
8
6
4
2
0
1/C² / x10¹¹ F⁻² cm⁴
2000 Hz
1000 Hz
500 Hz
-0.16 V
-0.6
-0.4
-0.2
0.0
0.2
0.4
0.6
0.8
1.0
Potential/ V vs RHE

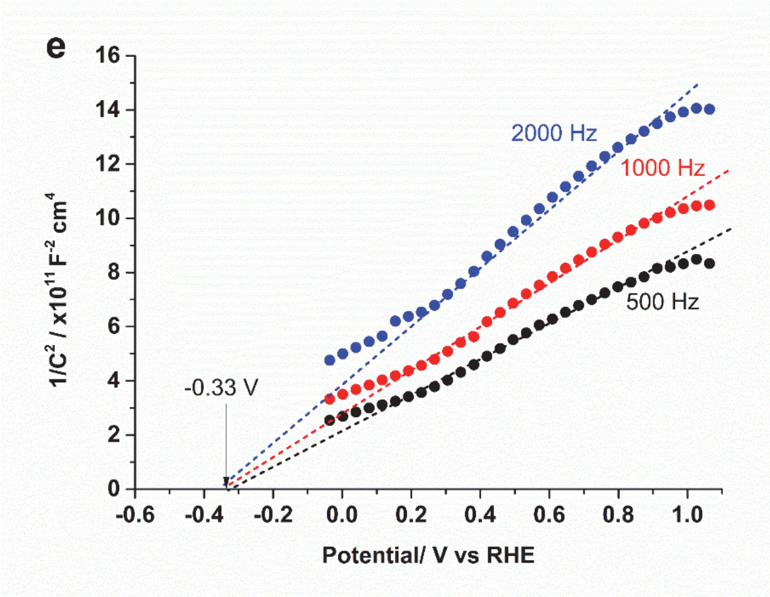

Figure S9. MS plot of a) Ta_3N_5, b) GaN/Al_2O_3, c) as-prepared Mg:GaN/ Al_2O_3, d) N_2 post annealed- Mg:GaN / Al_2O_3, e) NH_3 post annealed-Mg:GaN/ Al_2O_3.

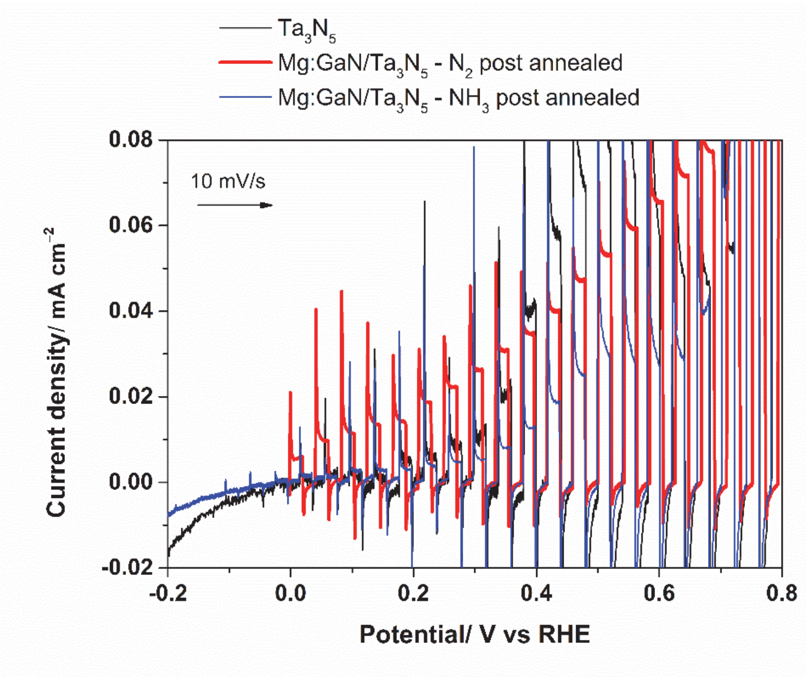

Figure S10. Magnification of background-subtracted LSV curve in Figure 5a, showing the onset potentials of Ta_3N_5 and Mg:GaN/Ta_3N_5 after N_2 and NH_3 post annealing.

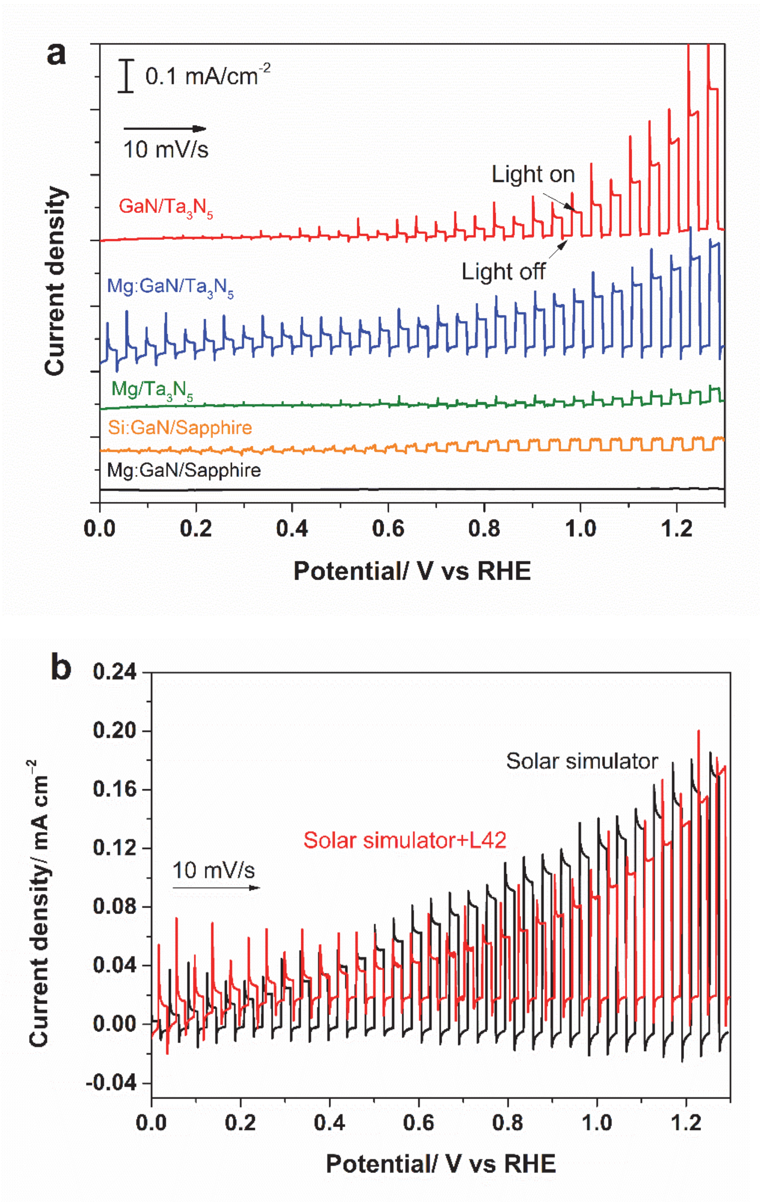

Figure S11. LSV of a) Si:GaN/sapphire, GaN/Ta_3N_5, Mg:GaN/Ta_3N_5 and Mg/Ta_3N_5, under full-light irradiation by solar simulator, b) Mg:GaN/Ta_3N_5 in solar simulator full light and solar simulator+L42 (visible light, λ>420 nm). All the experiments were done using 100 mL of 0.5 M K_2HPO_4 solution at pH 13 (KOH adjusted) electrolyte, with CoPi cocatalyst addition.

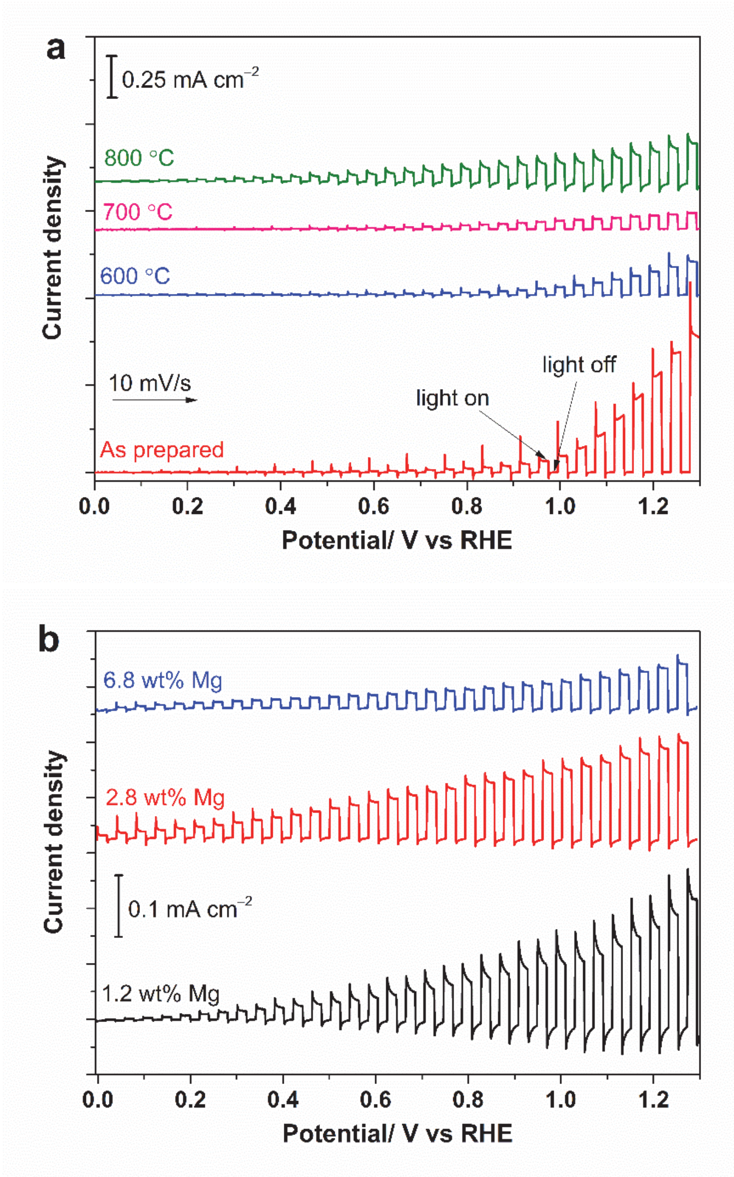

a
0.25 mA cm⁻²
800 °C
700 °C
600 °C
10 mV/s
light off
light on
As prepared
Current density
0.0
0.2
0.4
0.6
0.8
1.0
1.2
Potential/ V vs RHE
b
6.8 wt% Mg
2.8 wt% Mg
0.1 mA cm⁻²
1.2 wt% Mg
Current density
0.0
0.2
0.4
0.6
0.8
1.0
1.2
Potential/ V vs RHE

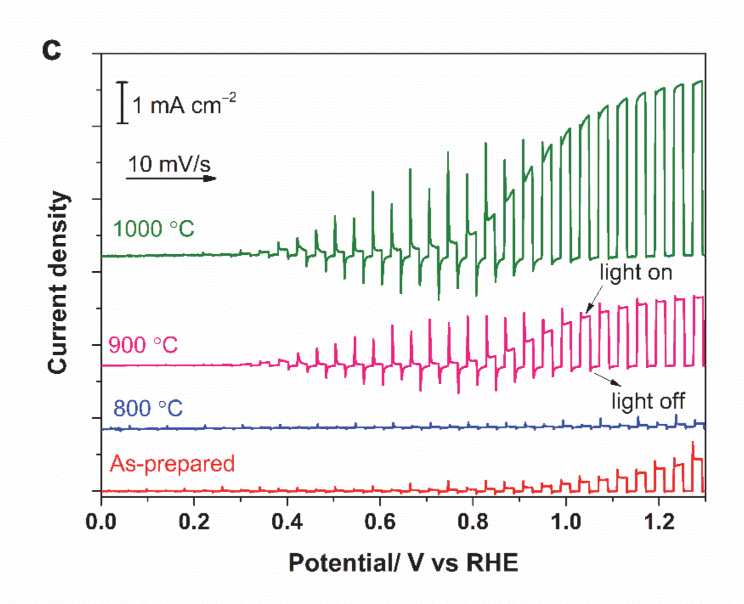
c
1 mA cm−2
10 mV/s
1000 °C
light on
900 °C
800 °C
light off
As-prepared
Current density
0.0
0.2
0.4
0.6
0.8
1.0
1.2
Potential/ V vs RHE

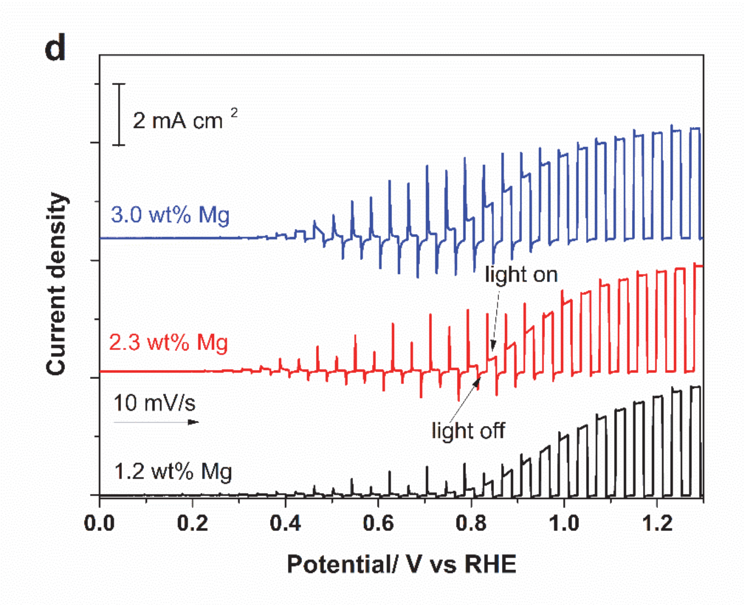
d
2 mA cm 2
3.0 wt% Mg
light on
2.3 wt% Mg
10 mV/s
light off
1.2 wt% Mg
Current density
0.0
0.2
0.4
0.6
0.8
1.0
1.2
Potential/ V vs RHE

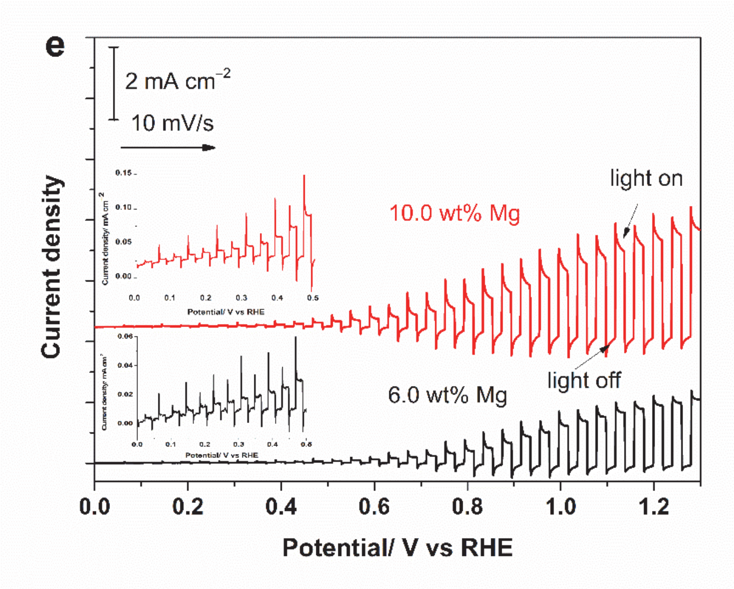

Figure S12. LSV of 100 nm Mg:GaN/Ta_3N_5 a) after N_2 post annealing with different temperatures, b) after N_2 post annealing at 800 °C with different Mg concentration, c) after NH_3 post annealing with different temperatures, d) after NH_3 post annealing at 1000 °C with different Mg concentration, e) 300 nm Mg:GaN/Ta_3N_5 after NH_3 post annealing.

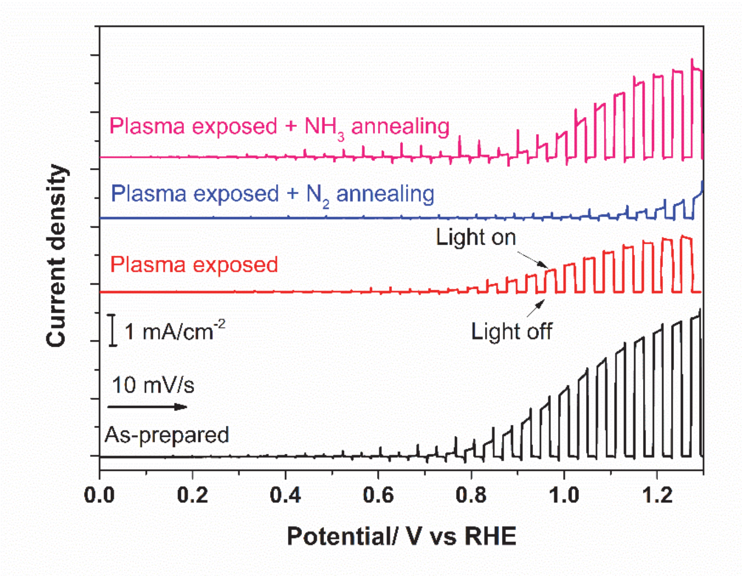

Figure S13. LSV of bare Ta_3N_5 exposed to PCVD chamber followed by N_2 or NH_3 post annealing.

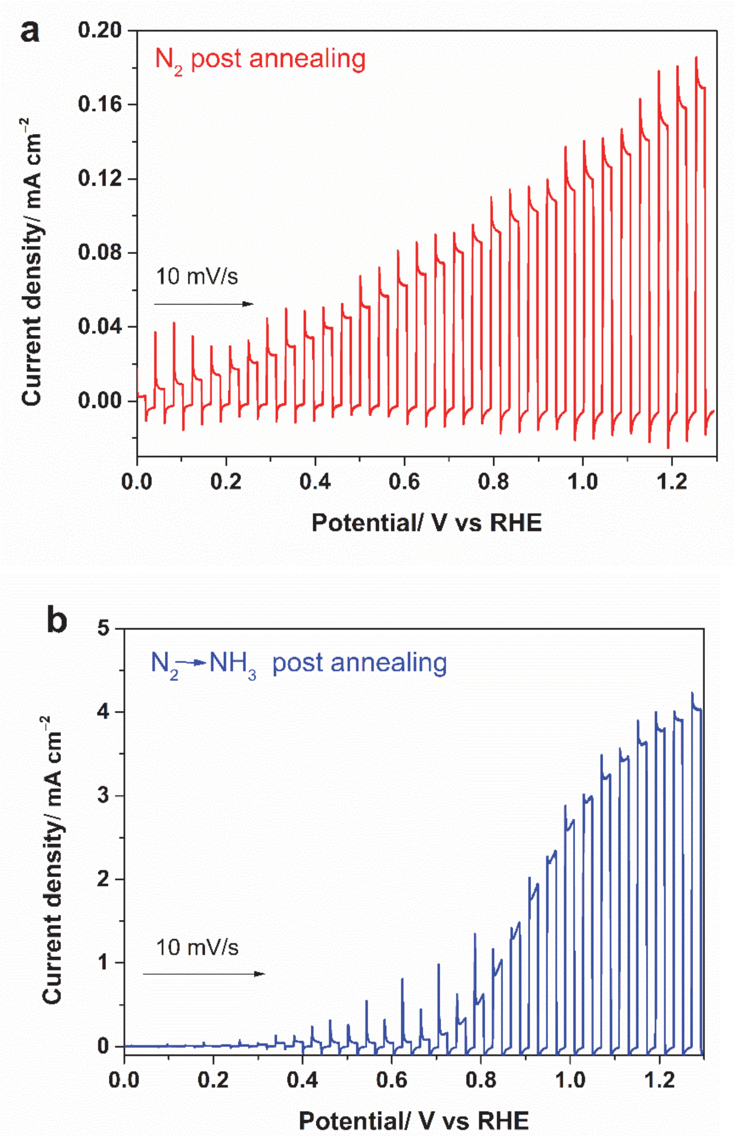

a
N_2 post annealing
10 mV/s
Current density/ mA cm^{-2}
Potential/ V vs RHE
0.20
0.16
0.12
0.08
0.04
0.00
0.0
0.2
0.4
0.6
0.8
1.0
1.2
b
$N_2 \rightarrow NH_3$ post annealing
10 mV/s
Current density/ mA cm^{-2}
Potential/ V vs RHE
5
4
3
2
1
0
0.0
0.2
0.4
0.6
0.8
1.0
1.2

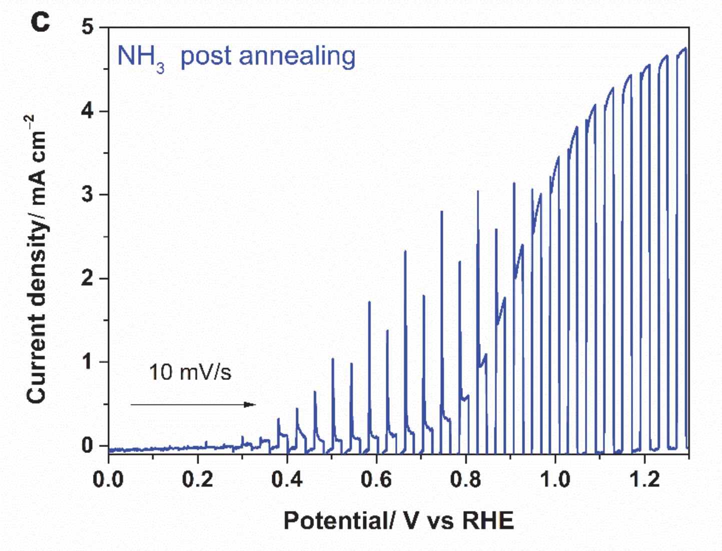

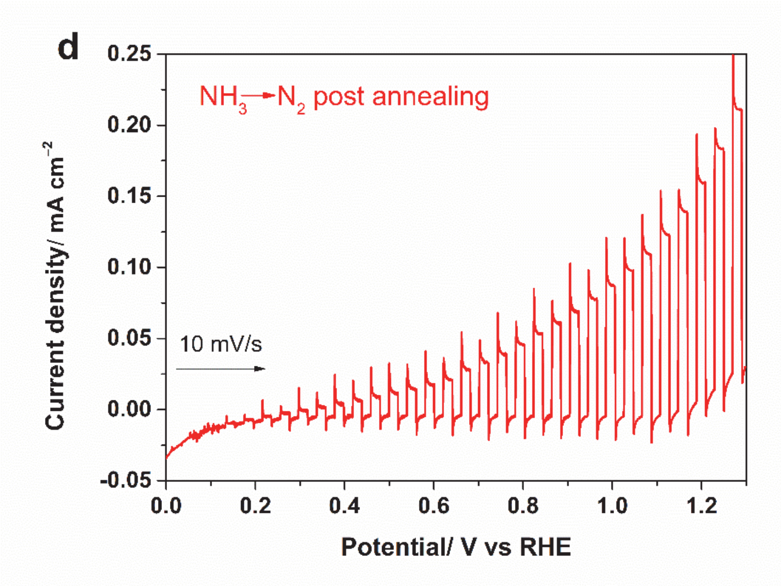

Figure S14. LSV of Mg:GaN/Ta_3N_5 subjected to a) N_2 post annealing, b) N_2 post annealing followed by NH_3 post annealing, c) NH_3 post annealing, d) NH_3 post annealing followed by N_2 post annealing.

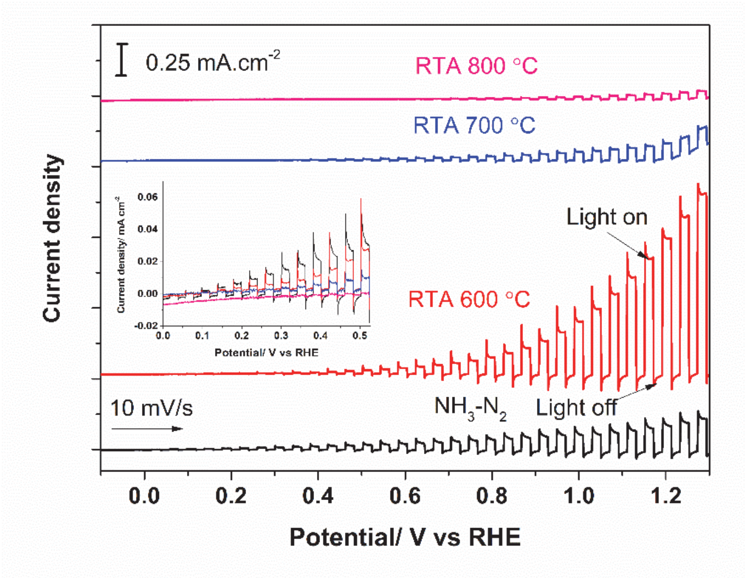

Figure S15. LSV of NH_3 post annealed-Mg:GaN/Ta_3N_5 sample followed by rapid thermal annealing (RTA) at different temperature in static N_2.